Phase and gain measurements in a distributed-loss cyclotron-resonance maser amplifier

Amit Kesar and Eli Jerby*
Tel-Aviv University, Ramat Aviv 69978, Israel

(Received 5 August 2001; revised manuscript received 6 December 2001; published 28 February 2002)

The control of gain and phase delay in a cyclotron-resonance maser (CRM) amplifier is essential for a variety of applications. In this experiment, the gain and phase-delay variations are measured with respect to controlling parameters; the electron-beam current and the axial magnetic field. Following Chu *et al.* [Phys. Rev. Lett. **74**, 1103 (1995)], the CRM amplifier comprises of a distributed-loss waveguide to enable high gain without oscillations. Our experiment yields an amplification up to 26 dB, and a phase-delay control range of 360°. In order to keep a fixed gain with the varying phase delay, the two controlling parameters (i.e., the solenoid field and the beam current) are operated together in a compensating mode. The experiment is conducted in a frequency of 7.3 GHz, with an electron beam of 18-kV voltage and 0.25–0.4-A current. The experimental results are compared with a theoretical model. Practical implementations of gain and phase control in CRM devices are discussed.

DOI: 10.1103/PhysRevE.65.036503 PACS number(s): 41.60.Cr, 84.40.Ik, 84.40.Ba

I. INTRODUCTION

Cyclotron-resonance masers (CRMs) and gyro-traveling-wave amplifiers, as presented in Ref. [1], are promising devices for high-power microwave amplification. The output power, gain, and bandwidth are fundamental characteristics of these devices. The feature of an inherent phase control in high-power microwave amplifiers could be useful for several future applications of existing and novel devices. This requires, however, a means to decouple the gain and phase variations. (For instance, keeping the gain level fixed while varying the phase delay.)

Phase control in high-power CRM amplifiers is essential for radiation beam-steering applications. The concept of CRM arrays and its implementations is presented in Ref. [2]. A particular application for an array of CRM amplifiers is the radiation beam steering, as an active phased-array antenna [3]. In this CRM synthesis, the simultaneous control of the gain and phase delay of each CRM-amplifier element is achieved by varying its electron-beam current and voltage. In such implementation the total radiated power is proportional to the number of CRM-amplifier elements in the array and to the output power of each element. The radiation pattern is shaped by the relative phase differences among the elements. If the control over the phase delay could be an inherent feature of the CRM amplifier, the need for external phase shifters could be alleviated. A similar angular steering method by free-electron laser array proposed in Ref. [4] was demonstrated by Cecere and Marshall [5].

Another CRM application proposed by Granatstein and Lawson [6,7] in which phase control could be essential is the use of gyroamplifiers and gyroklystrons as rf sources for driving particle accelerators. Inherent CRM features of phase control and phase stability may play an important role in these future applications.

The investigation of phase-delay variations in CRM gyro-amplifiers is essential not only for their incorporation in future schemes, which require inherent CRM phase-shifting abilities, but also for straightforward amplification purposes in which the phase stability is a major quality factor. Aspects of phase stability are studied in Refs. [8] and [9] for second-harmonic and frequency multiplying traveling-wave amplifiers, respectively.

Gyro-traveling-wave amplifiers tend to oscillate, in particular in high-gain operation, but Chu *et al.* [10] showed that these oscillations can be suppressed by a lossy section along the waveguide. The distributed wall losses in this section decay the oscillations but maintain the CRM amplification, whereas the following nonlossy section extracts the high output power. Using this concept, Chu *et al.* have obtained an ultrahigh gain (70 dB) at the *Ka* band [1].

In order to study the applicability of Chu's amplifier scheme as an element of the phased CRM-array active antenna, the dependence of its gain and phase delay on the operating parameters has been studied experimentally. The results are applicable for other possible applications as well.

This paper presents a gyroamplifier experiment implementing the distributed losses concept, in order to study its gain and phase-delay dependences on the electron-beam current and the axial magnetic field. The objectives of this study are (a) to demonstrate phase variation experimentally, (b) to verify the experimental results with theory, and (c) to prove that the gain and phase delay can be controlled independently, as predicted in Ref. [3].

II. EXPERIMENTAL SETUP

The CRM experimental scheme is shown in Fig. 1. The experimental operating parameters are listed in Table I. A linear electron beam is generated by an electron gun based on a thermionic cathode (Heatwave STD200). A cylindrical plate with a 5 mm diameter through a hole is placed 5 mm from the cathode to serve as an anode. The beam is focused by a focusing coil into the kicker section. The kicker consists of two plates of neodymium iron boron (NdFeB) permanent magnets. The magnets are attached to the wide waveguide

*Corresponding author. FAX: +972-3-6408048. Email address: jerby@eng.tau.ac.il

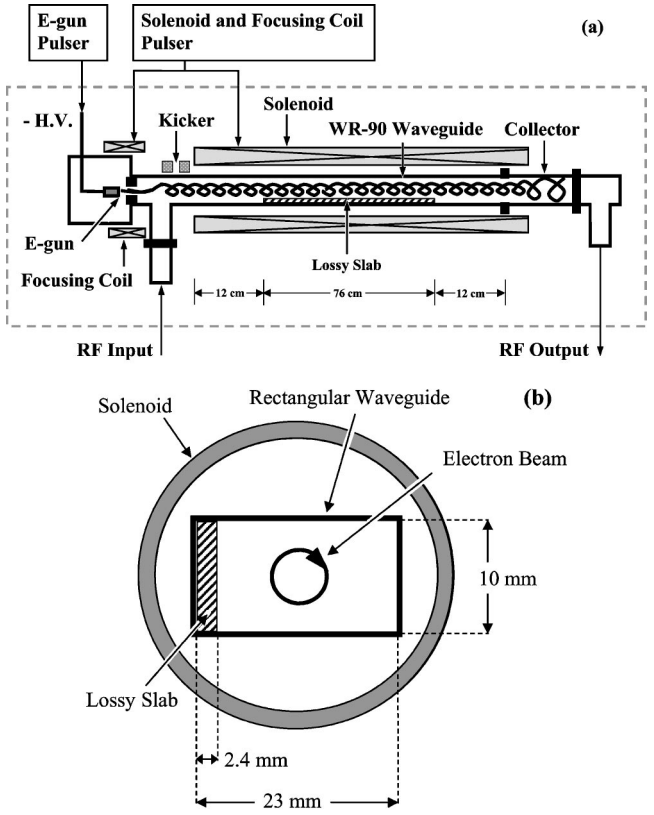

FIG. 1. CRM experimental scheme (a), and a cross section in the lossy waveguide section (b).

face and are poled into and out of it in the transverse direction. This kicker configuration resembles a wiggler's half period [11]. The electron gun and kicker are designed by the Herrmannsfeldt EGUN simulation code [12]. The electron-beam pitch ratio is found to be $\alpha \cong 1.3$ with a spread of $\Delta\alpha/\alpha \cong 12\%$. The beam is rotating in the cyclotron frequency along the axis of the WR90 rectangular waveguide. The axial magnetic field is produced by a 1.1-m-long solenoid.

The 1 m interaction length is succeeded by a 0.1-m waveguide extension operating as a collector. A lossy section of a 76-cm-long graphite slab (10.0×2.4 mm^2 cross section) is located in the center part of the interaction region, as shown

TABLE I. Experimental operating parameters.

Electron-beam voltage	18	kV
Electron-beam current	0.25–0.4	A
Kicker pitch ratio	1.3	
Pitch-ratio spread	7–12	%
Solenoid magnetic field	~2.5	kG
Cyclotron harmonic number	1	
Waveguide cross section	23×10	mm^2
Interaction length	100	cm
Lossy section length	76	cm
Loss factor	5	Np/m
Frequency	~7.3	GHz

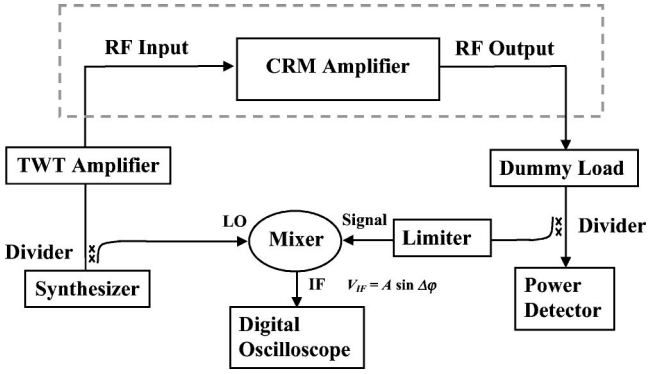

FIG. 2. Microwave diagnostic setup.

in Fig. 1(a). A transverse cross section of the CRM across the lossy waveguide section is shown in Fig. 1(b). The slab is attached to one of the narrow waveguide walls in order to suppress backward-wave CRM oscillations [13]. The waveguide insertion loss due to the lossy slab is 35 dB at the 7.3-GHz operating frequency.

The electron gun is fed by a 19-kV pulse generator. The solenoid and focusing coil are connected in series and fed by a current pulser. The maximal axial magnetic field is 2.7 kG, obtained in a pulse duration of ~4 ms.

The microwave diagnostic setup is shown in Fig. 2. The input signal (7.3 GHz, 1.6 W) is pulse modulated (6-μs pulse period, 80% duty cycle). It is produced by a synthesizer (HP 83752A) connected through a power divider to a TWT (traveling-wave tube) amplifier (Varian VZC-6960H1) and injected into the rf input port of the CRM. The input signal modulation enables one to verify at the output stage that the CRM operates indeed as an amplifier and that it does not oscillate.

The amplified output signal is dumped by a dummy load. A sampling of the output signal is split by a two arm power divider. One arm is connected to a crystal power detector (HP 423B) to measure the output power. The other arm is connected through a power limiter (MW-16300-SF-SF) to the signal port of a mixer (Magnum Microwave MM134P-1). The LO port of the mixer is fed by the rf synthesized generator (as shown in Fig. 2). The mixer IF output port voltage V_{IF} corresponds to the CRM phase delay by

$$V_{IF} = A \sin \Delta\varphi(t), \tag{1}$$

where A is a constant and $\Delta\varphi(t)$ is the time-dependent CRM phase delay. In this experiment the CRM phase delay is derived from the mixer output trace.

III. EXPERIMENTAL RESULTS

The CRM experimental setup described above was operated with the parameters listed in Table I. The measured beam voltage and current are 18 kV and 0.3 A, respectively. Figures 3(a)–3(c), show for instance, raw measurements of the solenoid field, the power detector, and the mixer output wave forms, respectively. It can be seen that during a 30 G fall of the solenoid field, the output power varies from 57 to 48 dBm, and the mixer IF output (1) accumulates one period

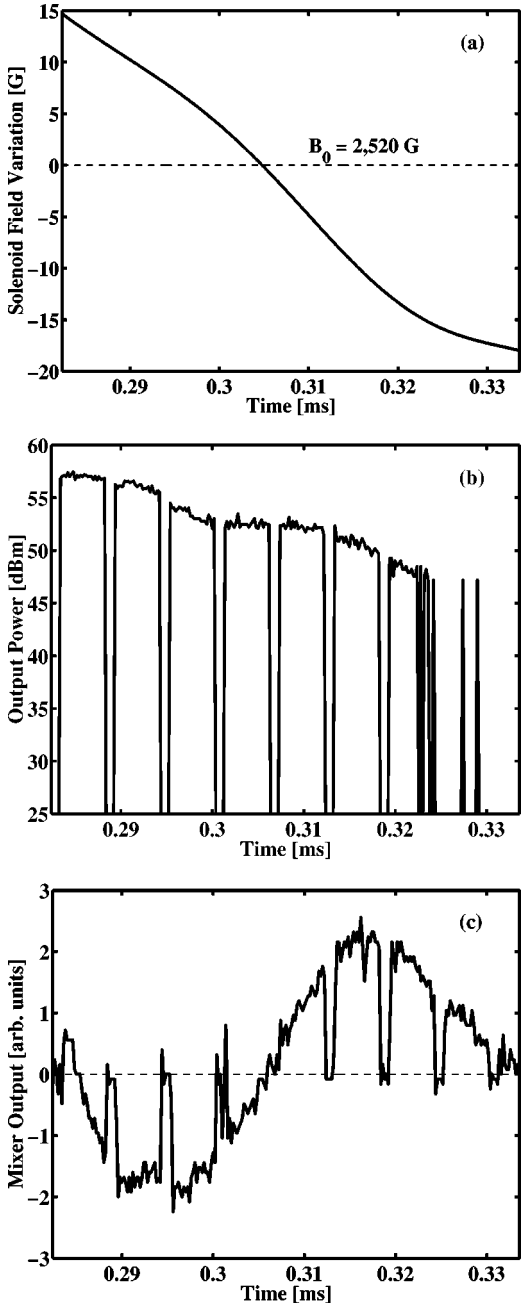

FIG. 3. Waveforms versus time of the axial magnetic field (a), power output (b), and mixer output (c).

of a sine wave. The power detector and mixer outputs are pulse modulated as the input signal, indicating a CRM amplification with no oscillations.

Figures 4(a)–4(d) show accumulated experimental results indicating the dependences of the power gain on the beam voltage, beam current, signal frequency, and solenoid field, respectively. The operating parameters are indicated in each figure by their specific ranges, whereas the common parameters are as listed in Table I. The dots indicate the maximum gain obtained within the specified parameter ranges. The dashed curves represent the second-order fit approximations of the experimental results. Figure 4(a) shows the linear tendency of the gain to increase with the beam voltage. Figure 4(b) shows that the gain attains a maximum for beam currents near ~ 0.3 A. Figure 4(c) shows the gain curve with respect to the signal frequency in the range of 7.15 to 7.40 GHz. Figure 4(d) shows the complementary dependence of the gain on a slight variation in the solenoid field in a fixed frequency (7.3 GHz). Both Figs. 4(c), 4(d) indicate a tuning bandwidth of $\sim 2.5\%$ for this CRM amplifier.

The experimental study of the CRM phase variation is supported by a theoretical analysis of the combined phase and gain dependences on the solenoid field and electron-beam current. This simultaneous dependence is calculated theoretically using the CRM nonlinear differential equations given in Ref. [14]. These equations are solved by the fourth-order Runge-Kutta method along the interaction axis for the CRM parameters listed in Table I. The intermediate lossy section is presented by an imaginary component ($k_z'' = 5$ Np/m) added to the axial wave number in order to simulate the waveguide distributed loss. The computed theoretical results are plotted in Fig. 5 as gain contours (solid lines) and phase-delay contours (dashed lines) versus the electron-beam current and solenoid field. The theoretical results show that a full 360° phase-delay range is achievable over a limited range of equigain contours.

Experimental measurements of the phase-delay dependence on the solenoid field are shown in Fig. 6 for a CRM gain of 19.5 ± 0.5 dBm and a 320 ± 5-mA electron-beam current. A phase variation of 0–180° is demonstrated in these conditions. The dashed line shows, for comparison, the theoretical results derived from Fig. 5 for the same conditions.

A full-cycle phase variation (0–360°) is demonstrated experimentally in Fig. 7 for a fixed gain (23.5 ± 0.5 dB) and a compensating electron-beam current (320 ± 40 mA) and voltage (18 ± 1 kV). The three-dimensional graph in Fig. 7 shows experimental results (circles) and their second-order best fit projections on the three perpendicular planes of this figure (in solid lines). For a comparison with the theoretical model, the corresponding computation results presented in Fig. 5 are shown with the experimental results of Fig. 7. The dashed curves on the $\Delta\varphi - I_{eb}$, $\Delta\varphi - \Delta B_0$, and $I_{eb} - \Delta B_0$ planes show these theoretical results. A considerable agreement between experiment and theory is acknowledged.

In view of recent advances in gyro-TWT studies for radar applications [15], there is an interest to characterize the features of this CRM amplifier in parametric terms related to radar and communication engineering. These characteristics include amplitude and phase modulation coefficients, spectral purity, phase linearity, and output noise, as investigated in Ref. [16]. In our CRM experiment, the amplitude modulation coefficients for the beam-current and solenoid-field variations are obtained from Figs. 4(b), 4(d) as ~ 0.12 dB/% and $\leqslant 5$ dB/%, respectively. These experimental outcomes agree with the theoretical result derived from Fig. 5.

The phase modulation (PM) coefficient for the beam current variation is derived theoretically from Fig. 5 as 0.9°/%. The PM modulation for the solenoid field variation is derived from the experimental results in Figs. 3(a), 3(c), as 220°/%, in agreement with the theoretical result from Fig. 5. Theoretical calculations of the CRM's bandwidth and phase linearity

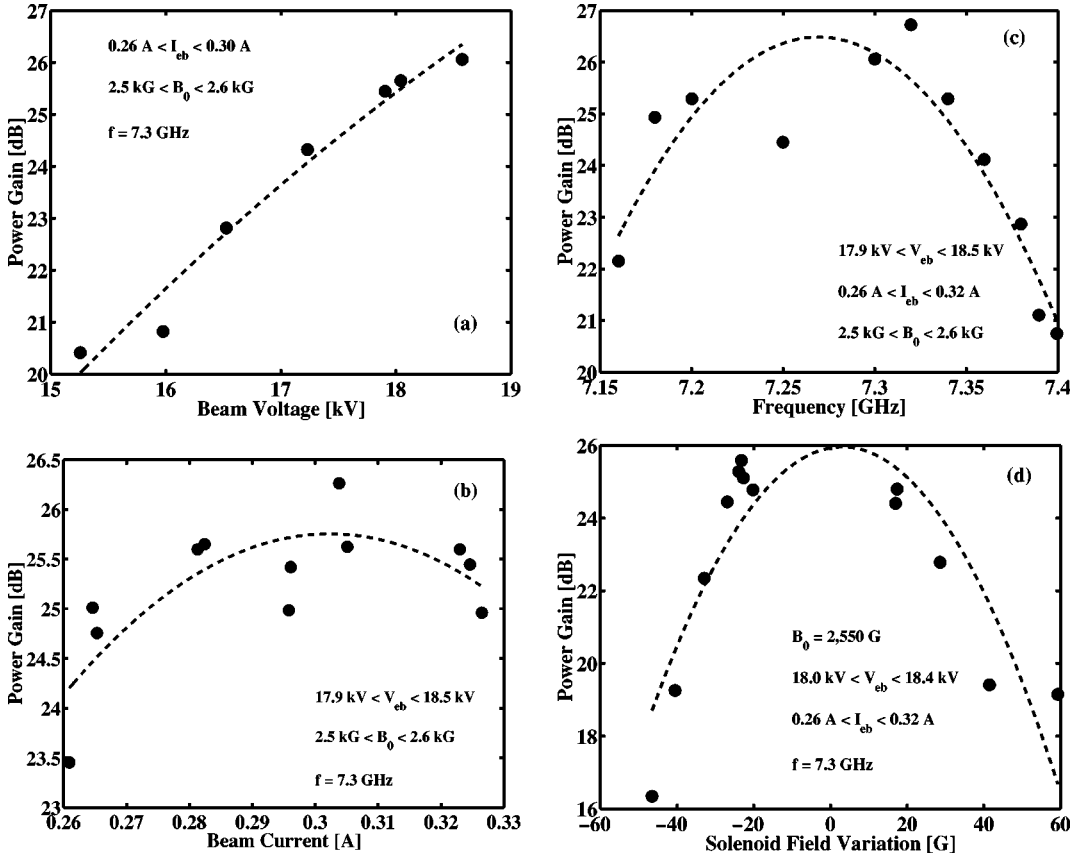

FIG. 4. Measurements of the power gain with respect to beam voltage (a), beam current (b), signal frequency (c), and solenoid field (d). The dots indicate the maximum gain obtained within the parameter ranges shown, and the dashed curves are their calculated second-order fits.

show an immediate bandwidth of 150 MHz (between -3 dB points), and a phase variation of $\pm 7°$ from the best-fit linear phase line within this frequency range.

Spectral purity measurements were obtained by mixing the CRM output signal (7.3 GHz, CW) with a local-oscillator signal at 7.35 GHz. The mixer IF output sampling was transformed to the frequency domain by a discrete Fourier transform. The spectral widening at the -10 dB points was found to be $\leqslant 40$ kHz with respect to the spectral width of the setup itself (230 kHz). The output noise, measured by a spectrum analyzer (HP 8592A) in the CRM's output port

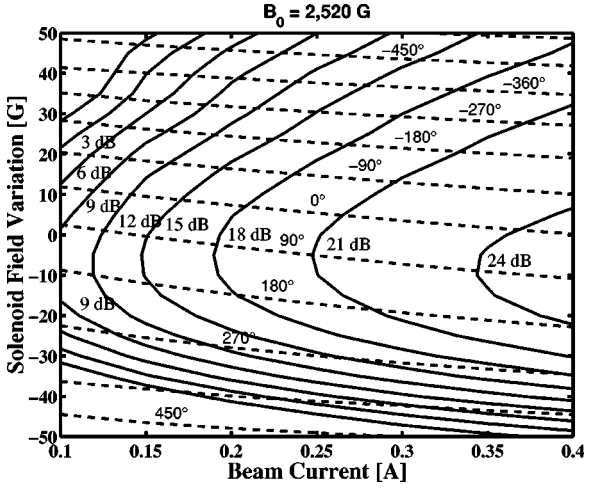

FIG. 5. A theoretical nonlinear computation of the CRM gain (solid contours) and phase delay (dashed contours) versus the electron-beam current and solenoid field variations around 2520 G. The operating parameters are listed in Table I.

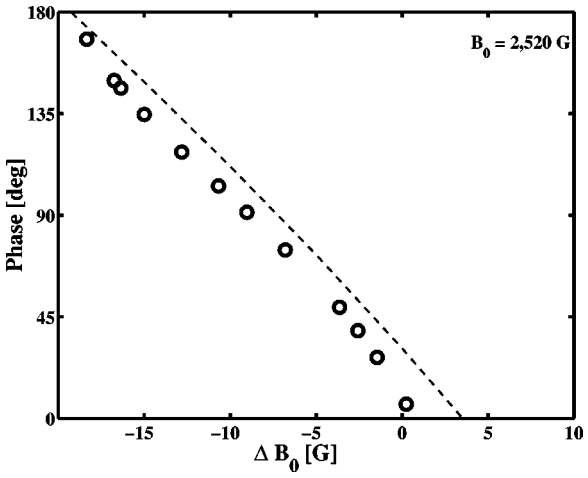

FIG. 6. Phase-delay measurements versus solenoid field for a 19.5 ± 0.5-dB gain and 320 ± 5-mA electron-beam current. The dashed line shows the theoretical result derived from Fig. 5 for the same conditions.

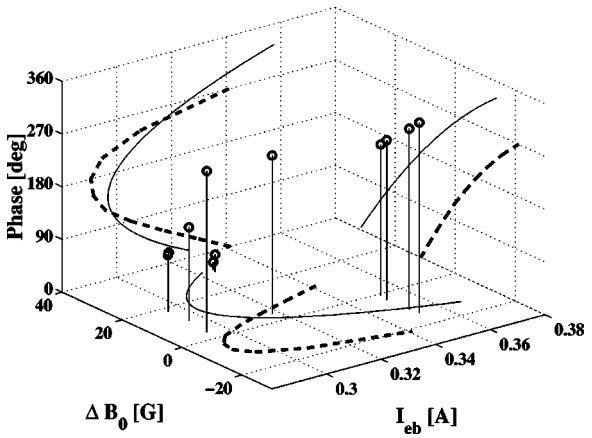

FIG. 7. Phase-delay measurements (shown by circles) versus electron-beam current and solenoid field for a 23.5 ± 0.5-dB gain. The solid curves on the perpendicular planes show the second-order best fits of the experimental results projections. The dashed curves show the theoretical results derived from the CRM model in Fig. 5 for the present conditions.

while the input port was terminated by a dummy load, was found to be -22.5 dB/MHz. This yields a 65.5 dB noise figure for the CRM's 26 dB gain.

IV. DISCUSSION

In this experiment, a distributed loss CRM amplifier [10] is operated at 7.3 GHz, with an 18-kV, 0.3-A electron beam. A maximum gain of 26 dBm is obtained with an 0.63 kW output power, and a 12% nonsaturated efficiency. This experiment extends the validity of the CRM distributed-loss concept to another operating regime than presented originally by Chu *et al.* [1,10].

Furthermore, the feasibility of uncoupled gain and phase-delay variations in a CRM amplifier is demonstrated experimentally. A full 360° phase-delay variation for a fixed CRM-gain is obtained experimentally, in agreement with theory (see Fig. 7). This result demonstrates, in principle, the feasibility of a phased-array active CRM antenna made of uncoupled distributed-loss CRM amplifier elements. Such an array requires a 360° variation range of an inherent CRM phase shift with an independently controlled gain [3]. This feature is demonstrated successfully in this experiment.

The simultaneous controllability of the phase delay by the electron-beam current and by the solenoid magnetic field is demonstrated experimentally and theoretically. Both agree within $\sim 4\%$ in the electron-beam current and $\sim 1\%$ in the solenoid magnetic field, and within a ± 0.5-dB gain margin. The electron pitch ratio and spread values were not measured in this experiment. In the CRM computation, we assumed electron pitch ratio and spread of $\alpha = 1.3$ and $\Delta\alpha/\alpha = 7\%$, respectively, though the EGUN simulations predicted the same pitch ratio with a higher spread ($\Delta\alpha/\alpha = 12\%$). This discrepancy has to be resolved in a future study.

The CRM amplifier characteristics such as amplitude and phase modulation coefficients, spectral purity, and phase linearity are evaluated in this study to be in a similar order of magnitude to the gyro-TWT scheme investigated by Ferguson *et al.* [16], but the noise figure found in our experiment is ~ 15 dB higher. Hence, these preliminary characteristics should be improved in order to enable the implementation of this CRM-amplifier scheme for radar and communication applications.

The gain and phase of the CRM amplifier, controlled here by the electron-beam current and solenoid field, can be implemented in practice as well. For instance, the electron-beam current can be controlled by a triode electron gun. Means to tune the static magnetic field can be incorporated even with permanent magnets [17,18], or in superconducting magnets [19]. In these CRM schemes, a magnetic field variation in the order of 1% is required for a full 360° cycle. This can be achieved by an additional low-current solenoid. In other CRM schemes, gain and phase controls can be implemented by the electron-beam voltage [3] or by the electron pitch-ratio variations.

The control over the phase delay could be essential as well for high-power gyroamplifiers and gyroklystrons designed to drive TeV linear colliders [6,7]. This feature could be used for an in-phase particle acceleration, to decrease phase jittering, and to stabilize CRM amplifiers.

Phase-controlled CRM amplifiers can be integrated in CRM arrays and operate as active phased-array antennas for high-power radars. The amplified signal can be radiated directly from each CRM-element aperture, while the proper phase and gain of each element are controlled by its electrical operating parameters, without the need for external (passive) phase shifters.

In view of the present experimental results, a further study towards practical implementations of phased-controlled CRM amplifiers based on the distributed-loss concept [1,10] should include: (a) a sensitivity analysis of the gain and phase-delay controllability with respect to all CRM operating parameters, including also beam voltage, electron spread, and interaction length, and (b) a phase jitter and stability analysis. For active CRM-array antennas, future studies should include (c) an analysis of the coupling between the CRM elements, and the influence of active reflections on the array performance, and (d) an experimental study of an active phased CRM-array antenna.

[1] K. R. Chu, H. Y. Chen, C. L. Hung, T. H. Chang, L. R. Barnett, S. H. Chen, T. T. Yang, and D. J. Dialetis, IEEE Trans. Plasma Sci. **27**, 391 (1999).

[2] E. Jerby, A. Kesar, M. Korol, L. Lei, and V. Dikhtiar, IEEE Trans. Plasma Sci. **27**, 445 (1999), and references therein.

[3] A. Kesar and E. Jerby, Phys. Rev. E **59**, 2464 (1999).

[4] E. Jerby, Phys. Rev. A **41**, 3804 (1990).

[5] M. Cecere and T. C. Marshall, IEEE Trans. Plasma Sci. **22**, 654 (1994).

[6] V. L. Granatstein and W. Lawson, IEEE Trans. Plasma Sci. **24**,

648 (1996).
[7] W. Lawson, M. Castle, S. Gouveia, V. L. Granatstein, B. Hogan, G. Nusinovich, M. Reiser, and I. Spassovsky, in *Proceedings of the 25th International Conference on Infrared and Millimeter Waves*, edited by S. Liu and X. Shen (IEEE, Piscataway, New Jersey, 2000), pp. 107–108.
[8] Q. S. Wang, D. B. McDermott, and N. C. Luhmann, Jr., IEEE Trans. Plasma Sci. **24**, 700 (1996).
[9] G. S. Nusinovich, J. Rodgers, W. Chen, and V. L. Granatstein, IEEE Trans. Electron Devices **48**, 1460 (2001).
[10] K. R. Chu, L. R. Barnett, H. Y. Chen, S. H. Chen, Ch. Wang, Y. S. Yeh, Y. C. Tsai, T. T. Yang, and T. Y. Dawn, Phys. Rev. Lett. **74**, 1103 (1995).
[11] V. L. Bratman and S. V. Samsonov (private communication).
[12] W. B. Herrmannsfeldt, computer code EGUN—an electron optics and gun design program (Stanford Linear Accelerator Center, Stanford University, Stanford, California, 1988).
[13] K. R. Chu (private communication).
[14] G. S. Nusinovich and M. Walter, Phys. Plasmas **4**, 3394 (1997).
[15] K. T. Nguyen, J. P. Calame, D. E. Pershing, B. G. Danly, M. Garven, B. Levush, and T. M. Antonsen, Jr., IEEE Trans. Electron Devices **48**, 108 (2001).
[16] P. E. Ferguson, G. Valier, and R. S. Symons, IEEE Trans. Microwave Theory Tech. **29**, 794 (1981).
[17] T. Kikunaga, H. Asano, Y. Yasojima, F. Sato, and T. Tsukamoto, Int. J. Electron. **79**, 655 (1995).
[18] D. B. McDermott, A. J. Balkcum, and N. C. Luhmann, Jr., IEEE Trans. Plasma Sci. **24**, 613 (1996).
[19] K. Koppenburg, G. Dammertz, M. Kuntze, B. Piosczyk, and M. Thumm, IEEE Trans. Electron Devices **48**, 101 (2001).